An exceptionally well-preserved skeleton of *Palaeothentes* from the Early Miocene of Patagonia, Argentina: new insights into the anatomy of extinct paucituberculatan marsupials

Analia M. Forasiepi · Marcelo R. Sánchez-Villagra · Thomas Schmelzle · Sandrine Ladevèze · Richard F. Kay

Abstract During the Cenozoic paucituberculatans were much more diverse taxonomically and ecomorphologically than the three extant genera of shrew-like marsupials. Among paucituberculatans, palaeothentids were abundant during the Early Miocene, although most of the fossil remains consist of isolated teeth or fragmentary jaws. We describe a new and exceptional partial skeleton of *Palaeothentes lemoinei* (Palaeothentidae), collected from the Santa Cruz Formation (Santacrucian age, Early Miocene) in Patagonia. Whereas the skull of *P. lemoinei* has more plesiomorphic traits in the face, palate, and cranial vault than that of living paucituberculatans, the dental morphology is more derived. The osseous inner ear was examined using micro-CT scanning, revealing a cochlea with 1.9 turns, the presence of a "second crus commune", an anterior semicircular canal (SC) projecting slightly dorsally from the dorsal-most point of the posterior SC, and lateral and posterior SCs projecting laterally to the same level. On the basis of postcranial anatomy, previous studies have demonstrated that *P. lemoinei* was an agile cursorial form, an inference supported by study of the new postcranial elements.

Keywords Marsupialia · Metatheria · Cenozoic · South America · Skull · Inner ear · Postcranium

A. M. Forasiepi
Instituto Argentino de Nivología, Glaciología y Ciencias Ambientales, CCT-Mendoza, CONICET, Av. Ruiz Leal s/no, 5500 Mendoza, Argentina

A. M. Forasiepi · M. R. Sánchez-Villagra (✉)
Palaeontological Institute and Museum, University of Zürich, Karl Schmid-Strasse 4, 8006 Zürich, Switzerland
e-mail: m.sanchez@pim.uzh.ch

T. Schmelzle
Fleckensteinstraße 7, 74206 Bad Wimpfen, Germany

S. Ladevèze
Muséum national d'Histoire naturelle, UMR 7207 CR2P CNRS/MNHN/UPMC, 8, rue Buffon, CP38, 75231 Paris Cedex 05, France

R. F. Kay (✉)
Department of Evolutionary Anthropology, Duke University, Durham, NC 27708-03083, USA
e-mail: richard.kay@duke.edu

Abbreviations

Institutional abbreviations

FMNH	Field Museum of Natural History, Chicago, USA
IEEUACH	Universidad Austral de Chile, Instituto de Ecología y Evolución, Valdivia, Chile
MACN-A	Museo Argentino de Ciencias Naturales "Bernardino Rivadavia", Ameghino Collection, Buenos Aires, Argentina
MNHN-Pal-Bol-V	Museo Nacional de Historia Natural, Vertebrates, La Paz, Bolivia
MPM-PV	Museo Regional Provincial "Padre M. Jesús Molina", Río Gallegos, Argentina
PU	Princeton University collections at Yale University, USA

Anatomical abbreviations

I/i	Upper and lower incisor
C/c	Upper and lower canine
P/p	Upper and lower premolar

🖄 Birkhäuser

M/m   Upper and lower molar
ASC   Anterior semicircular canal
LSC   Lateral semicircular canal
PSC   Posterior semicircular canal

Introduction

Paucituberculata is a clade of shrew-like marsupials endemic to South America. The group includes seven extant small and insectivorous species arranged in three genera: *Caenolestes*, *Lestoros,* and *Rhyncholestes* (Wilson and Reeder 1993; Ojala-Barbour et al. 2013). Fossil members of this group were much more diverse taxonomically and ecomorphologically (Marshall 1980; Bown and Fleagle 1993; Abello 2007; Abello and Candela 2010) and are known since the Early Eocene (Itaboraian age) (Goin et al. 2009; Abello 2013; Fig. 1).

The alpha taxonomy and the phylogenetic relationships of paucituberculatans has been thoroughly revised (Abello 2007, 2013) and continues to be studied (Goin et al. 2010; Abello and Rubilar-Rogers 2012). The discovery of early paucituberculatans and closer relatives (Goin et al. 2007, 2009; Forasiepi et al. 2013) significantly increases the understanding of the character evolution within this clade. Several studies based on molecular, morphological, and combined data agree that paucituberculatans are the sister taxa of Australidelphia (e.g., Horovitz and Sánchez-

Villagra 2003; Asher et al. 2004; Nilsson et al. 2004, 2010; Beck et al. 2008; Horovitz et al. 2008, 2009; Meredith et al. 2008). Other studies located paucituberculatans at the base of Marsupialia (e.g., Szalay 1994; Baker et al. 2004; Meredith et al. 2009, 2011) or provided the two alternatives (Beck 2008). Consequently, the understanding of the anatomy of fossil paucituberculatans has the potential to provide new data to interpret the anatomy and the character evolution of the Australian marsupials or early marsupials. Unfortunately, the fossil record of paucituberculatans is mainly confined to teeth.

Paucituberculatans are typically classified into the Linnaean families Caenolestidae, which includes the living taxa, and the extinct Pichipilidae, Abderitidae and Palaeothentidae, and stem taxa (Marshall 1980; Bown and Fleagle 1993; Abello 2007, 2013; Goin et al. 2009; Abello 2013; Fig. 1). Palaeothentidae occurred from the late Oligocene to the middle Miocene (Deseadan to Laventan ages) in Colombia, Bolivia, southern Argentina, and Chile (Marshall 1980; Bown and Fleagle 1993; Dumont and Bown 1997; Abello 2007, 2013). Palaeothentids were abundant during the late Early Miocene (Santacrucian age), with *Palaeothentes* being the most speciose genus, with five species: *P. aratae, P. intermedius, P. lemoinei, P. minutus,* and *P. pascuali.* Despite an extensive fossil record, complete skulls and skeletons are rare. Most of the fossil remains consist of isolated teeth, fragmentary mandibles and fragmentary maxillae (Abello 2007). To date, four
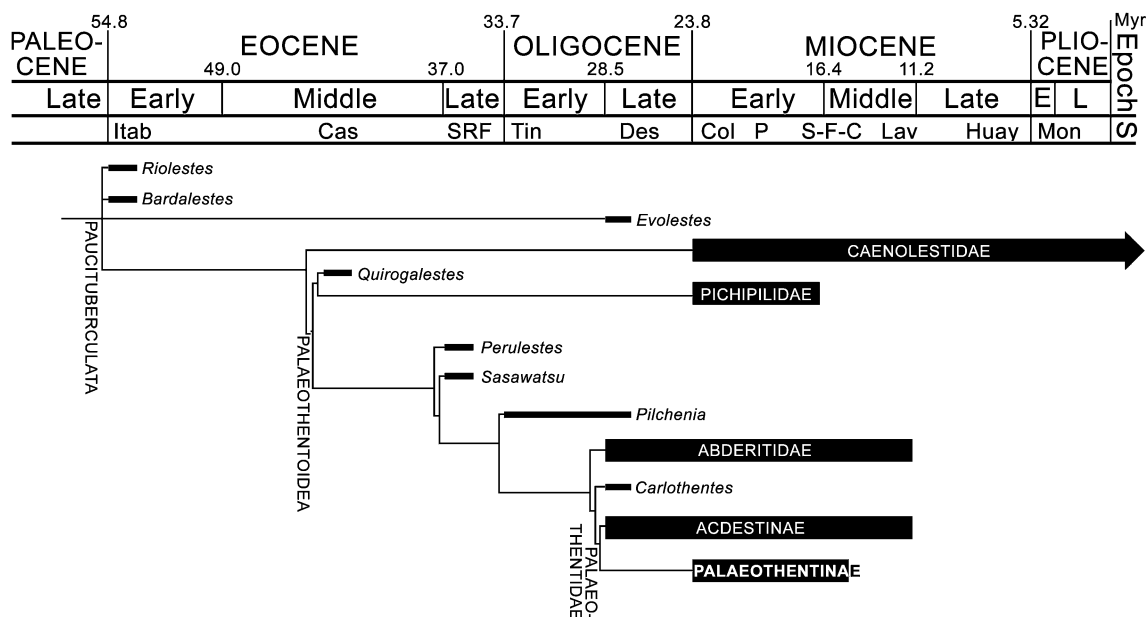

Fig. 1 Phylogenetic relationships of several paucituberculatans based on Abello (2013), indicating Palaeothentinae (the monophyletic group to *Palaeothentes lemoinei* belongs) in *bold upper case*. South American Land Mammal Ages (*S*) are as follows (from older to younger): *Itab* Itaboraian, *Cas* Casamayoran, *SRF* Santa Rosa Fauna, *Tin* Tinguiririran; *Des* Deseadan, *Col* Colhuehuapian, *P* Pinturan fauna; *S–F–C* Santacrucian, Friasian, and Colloncuran, *Lav* Laventan, *Huay* Huayquerian, *Mon* Montermosan

skulls of palaeothentids have been described. One belongs to the Santacrucian palaeothentid *Palaeothentes minutus* (MACN-A 8271), and was damaged subsequent to its illustration by Ameghino (1887, p. 6; see also Marshall 1980, fig 20). Two other partial skulls assignable to the acdestid *Acdestis oweni* are also from the Santacrucian: specimens PU 15225 and FMNH 13160, the former described by Sinclair (1906) as *Palaeothentes intermedius* and referred to *Acdestis spegazzinii* by Abello (2007). The fourth skull is from rocks of Laventan age of Bolivia (MNHN-Pal-Bol-V-4000) and was described as *Acdestis maddeni* (Goin et al. 2003).

This contribution describes and examines a new specimen, comprising the skull and postcranial skeleton, of the palaeothentid *P. lemoinei* (MPM-PV 3566), collected from Puesto Estancia La Costa of the Estancia La Costa Member, Santa Cruz Formation (Santacrucian age). The specimen was recovered in 2003 by RFK during a joint expedition from Museo de la Plata (Argentina) and Duke University (USA). This new specimen adds insights into the knowledge of the anatomy of extinct paucituberculatans and is the core of the present study, focusing on the middle ear anatomy. We apply the techniques of CT technology to study the internal osseous inner ear anatomy of *P. lemoinei* and to undertake comparisons with other Metatheria.

Materials and methods

The nomenclature for the descriptions follows veterinary text books (e.g., Schaller 1992) and particular publications based on metatherians. The nomenclature for the skull follows Wible (2003), for the petrosal Wible (1990, 2003), for the inner ear Schmelzle et al. (2007), and for the dentition Abello (2007, 2013).

The internal structure of the petrosal bone of *P. lemoinei* was documented using a micro-CT-Scanner RayScan 200 at the Fachhochschule Aalen, Germany. *Caenolestes* sp. was scanned at the Anthropological Institut and Museum of the University of Zürich, (μCT80, Scanco Medical, Bassersdorf). The specimen of *Dromiciops gliroides* (IEEU-ACH 2167) was scanned at the University of Poitiers (X8050-16 Viscom μCT scan). The resulting graphic files were used to reconstruct the inner ear three-dimensionally using Avizo 8, VGStudio Max 1.1® and Materialise Mimics 16® (licence UMR7207). In order to generate a virtual cast of the inner ear, a negative of the file was produced and the software Cinema 4d® R8 XL (Losch et al. 1999) was used to delete the reconstructed areas of the petrosal bone that cover the bony labyrinth. For *Caenolestes* sp. and Dromiciops gliroides, the left petrosal was scanned but Figure 7 shows the mirrored inner ear for

easier comparison. For the description, the lateral semi-circular canal was oriented horizontally and at the centre of the anatomical structures (Graf and Klam 2006). The turns of the cochlea were counted following the protocol of West (1985).

Systematic palaeontology

Marsupialia Illiger 1811
Paucituberculata Ameghino 1894
Palaeothentidae Sinclair 1906
Palaeothentes Ameghino 1887
P. lemoinei Ameghino 1887

Holotype. MACN-A 3, fragment of right dentary with m1–m4.

Occurrence and age. Santa Cruz, Pinturas, and Río Frias formations, Early–Middle Miocene (Santacrucian–Friasian South American Land Mammal Ages), Patagonia, Argentina and Chile (Marshall 1980, 1990; Bown and Fleagle 1993; Abello 2007).

Referred specimen. MPM-PV 3566, skull with dentition, complete left and fragment of right dentary with dentition, right petrosal, and postcranium (16 vertebrae, ribs, right pelvic girdle, right femur, proximal fibula, right astragalus, left humerus, left ulna, both radii, metapodials, and phalanxes).

Remarks. The combination of the following features permits allocation of MPM-PV 3566 to *P. lemoinei* (for a taxonomic revision of the genus and revised diagnosis see Abello 2007): wide crown bases in M1–M2, larger in molar size than the Santacrucian species *P. intermedius, P. pascuali,* and *P. minutus* and smaller than in *P. aratae* (Abello 2007; Tables 18a–d), less steep molar-size gradient from m1 to m4, and more protruding protocone on M1. Additionally, *P. lemoinei* has the plesiomorphic traits of P1 with two roots (unirradiculated in *P. aratae*) and a proportionally smaller m1 trigonid, and its corresponding P3 counterpart (larger in *P. aratae*).

Description and comparisons

Skull

The skull is complete except for missing most of the right zygomatic arch, the anterior-most portion of the nasals, and the posterior portion of the basicranium (Fig. 2). The skull preserves most of the upper dentition and portions of the ear region, including an isolated right petrosal bone.

Compared to extant paucituberculatans (*Caenolestes*: mean for the different species range from 31 to 37 mm—Ojala-Barbour et al. 2013—, *Lestoros*, mean about

Fig. 2 Palaeothentid marsupial *Palaeothentes lemoinei* (MPM-PV 3566), from the late Early Miocene, Santa Cruz Formation, Patagonia, Argentina. Skull in dorsal (**a**), ventral (**b**), and lateral (**c**) views. *Scale bar* 10 mm

30 mm—Martin 2013—, and *Rhyncholestes*, mean about 33 mm—Osgood 1924; Patterson and Gallardo 1987), the skull of *P. lemoinei* is much larger and with a shorter and wider snout (Table 1). In lateral view, the premaxilla makes a large contribution to the anterior part of the snout, as in other paucituberculatans, with a facial process that represents more than 35 % of the total length of the snout (Fig. 2c). The most distal part of the premaxilla is broken, although the facets on the maxilla suggest that the facial process of the premaxilla is wedged between the maxilla and nasal and projects posteriorly to the level of P2. As in other palaeothentids, there is no trace of an antorbital

Table 1 Measurements of the skull and dentary (in mm)

Skull	
Total (condylobasal) length	63[a]
Maximum midline palatal length	39
Interorbital constriction width	7.8
Maximum palate width (between lingual the side of M1)	12.3
Dentary	
Maximum length	38.5[a]
Height at the level of the condylar process	10.2
Height at the level of the coronoid process	20.2

[a] The measurement is approximated

vacuity between the nasal and maxilla (Sinclair 1906; Goin et al. 2003), a difference from caenolestids (Dederer 1909; Osgood 1921; Martin 2013). The remaining part of the snout is completed by the maxilla. A large infraorbital foramen opens on the facial process and is located at the level of the posterior root of P3. The maxilla contacts the frontal, in common with several stem marsupials (e.g., *Pucadelphys*, *Herpetotherium*; Marshall and Muizon 1995; Horovitz et al. 2008) and most living marsupials. The maxilla-jugal suture is nearly vertical. The zygomatic arch is deep dorsoventrally and robust, differing from the slender arch found in caenolestids. The anterior root of the zygoma is formed by the short zygomatic process of the maxilla.

In dorsal view (Fig. 2a), the nasals are narrow, although less so than in living caenolestids (Osgood 1921; Martin 2013). The nasals widen gradually posteriorly. The suture between nasals and frontals is W-shaped, with the frontal forming an anterior wedge.

In ventral view (Fig. 2b), the palate is narrow anteriorly and wide at the level of M1–M2, with the molars arranged in arch. The anteriormost margin of the incisive foramen is missing (Fig. 3a), but it is evident that this foramen was large, similar to that of living caenolestids, with its posterior margin on the maxilla extending caudally to the posterior border of P1 (Fig. 3b). The major palatine foramen is contained in an extensive maxillopalatine vacuity, although smaller than in living caenolestids (Osgood 1921; Patterson and Gallardo 1987; Martin 2013). This vacuity extends from the level of the M1–M3. Posteriorly and at the level of M4, there is another pair of small apertures, the posteromedial or palatine vacuity sensu Hershkovitz (1997) opening close to the midline of the palate. The palate extends behind the M4. The posterior border of the palate is straight and strengthened by the palatine torus (Fig. 2b). In lateral view (Fig. 2c), the facial process of the lacrimal is small and restricted to the orbital rim. A single lacrimal foramen was observed right by the orbital rim, as in living caenolestids (Dederer 1909; Osgood 1921; Martin 2013). The postorbital constriction, as observed in dorsal view (Fig. 2a), is deep, similar to the fossil palaeothentids *Acdestis maddeni* (Goin et al. 2003) and *Acdestis oweni* (Sinclair 1906) and differing from living caenolestids, which have a very shallow constriction. The preorbital area is wide, as in other palaeothentids (Sinclair 1906; Goin et al. 2003), and comparable to the width of the braincase. This differs from living caenolestids, which have broader and more globular braincases. The temporal lines are low and short, lacking contact with the sagittal crest (Fig. 2a). In *P. minutus* (Sinclair 1906), the temporal lines are stronger than in *P. lemoinei*; in contrast, living caenolestids lack these structures. In *P. lemoinei*, the sagittal crest extends on the midline of the skull, including frontals and parietals, from the level of the postorbital constriction to the nuchal crest. The nuchal crests are tall and posteriorly projecting. The sagittal and nuchal crests are well defined in fossil palaeothentids (Sinclair 1906; Goin et al. 2003). In contrast, living caenolestids have no crests in this area of the skull. An interparietal is not an independent bone in *P. lemoinei*, or any other adult caenolestids. It is likely fused to the parietals as this bone was found to be universal among mammals (Koyabu et al. 2012). The mid-frontal and mid-parietal sutures are partially observed, contrary to adult and subadult Recent caenolestids in which these sutures are fused (Voss and Jansa 2009).

The basisphenoid and alisphenoid are partially preserved (Fig. 2b). The carotid foramen opens latero-ventrally, just anterior to the suture with the basioccipital, in a manner similar to *A. maddeni* (Goin et al. 2003). The opening is large and oval. The transverse canal foramen is situated just anterior and lateral to the carotid foramen, as in most marsupials including caenolestids (Sánchez-Villagra and Wible 2002). The alisphenoid tympanic process is prominent and makes a contribution to the ossified auditory bulla. Its contact with the rostral tympanic process of the petrosal, present in *Caluromys* and *Caluromysiops* (Voss and Jansa 2009), is not possible to determine because the petrosal was preserved detached from the skull. The foramen ovale is bordered anteriorly by the alisphenoid. Because of incomplete preservation, it is not possible to determine whether the foramen ovale was bordered by both the alisphenoid and the petrosal, as in most marsupials including extant caenolestids, or if the foramen was entirely contained within the alisphenoid (e.g., Sánchez-Villagra 2001; Voss and Jansa 2009). In posterior view, the occipital area is flat, not globular as in living caenolestids.

Petrosal. The mammalian petrosal has two main divisions: the pars cochlearis, enclosing the auditory organ (the cochlea), and the pars canalicularis, housing the organs of the balance (the vestibular system) (Wible 2003). In tympanic view (Figs. 4a, 5a), the pars cochlearis is represented by the promontorium and anteromedial flange, while the pars canalicularis is represented by the bone posterior and lateral to the promontorium. The promotorium is bulbous and lacks grooves for vascular canals. The rostral tympanic process is a short crest, concave laterally and taller posteriorly, as in *Acdestis maddeni* (Goin et al. 2003). However, the ridge of this crest-like process has a minimum of five small tubercles plus additional, smaller ones that are absent in *A. maddeni*. The rostral tympanic process of *P. lemoinei* differs from the protruding finger-like process of didelphids (Wible 2003) and even the low process of *Caenolestes* (Sánchez-Villagra and Wible 2002). The anteromedial flange projects from the promontorium. This is a flat shelf in tympanic view, wider at its posterior base. The most anterior portion of this shelf is broken. The shallow

Fig. 3 *Palaeothentes lemoinei* (MPM-PV 3566). Details of the premaxilla (**a**) and palate (**b**) with the upper dentition. *Scale bar* 5 mm (**a**) and 10 mm (**b**)
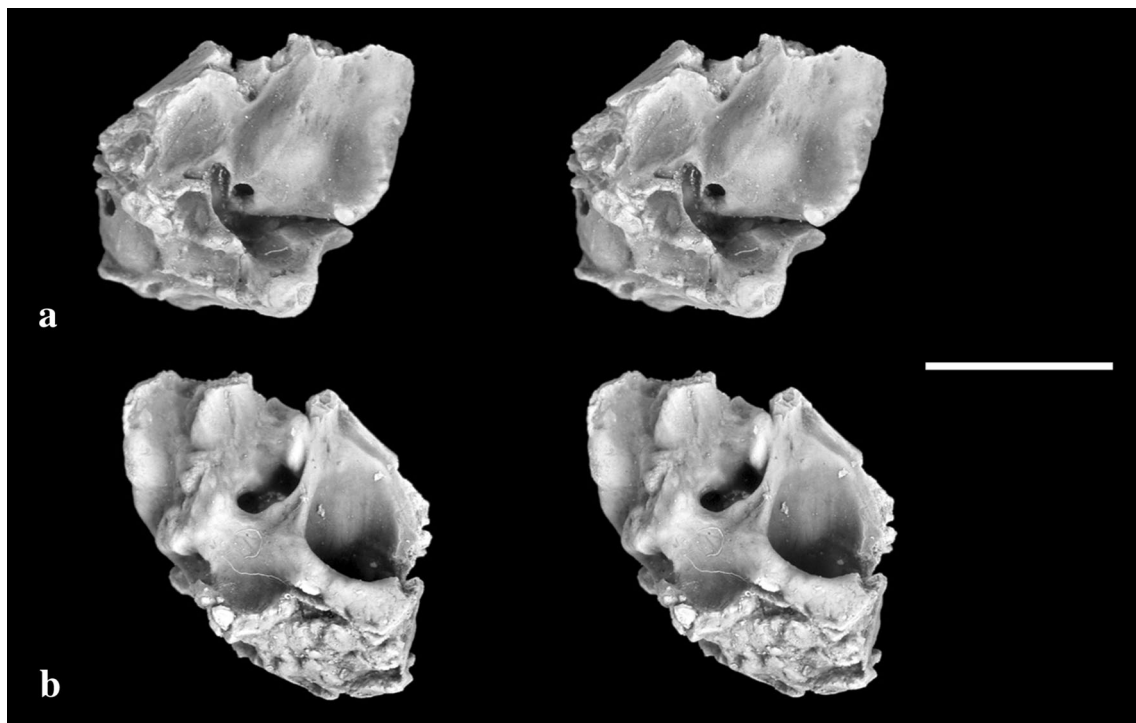

Fig. 4 *Palaeothentes lemoinei* (MPM-PV 3566). Stereo pairs of the right petrosal in tympanic (**a**) and cerebellar (**b**) views. *Scale bar* 5 mm

elongated depression located lateral to the anteromedial flange is recognised as the tensor tympani fossa for attachment of the tensor tympani muscle (Wible 2003).

Three main apertures are located posterior and lateral to the promontorium: the fenestra cochleae posteromedially, the fenestra vestibuli posterolaterally, and the secondary facial foramen laterally. The fenestra cochleae, for the attachment of the secondary tympanic membrane, opens on the posterior wall of the promontorium and is partially hidden in tympanic view by the tall and robust caudal tympanic process (Figs. 4a, 5a). The fenestra vestibuli opens anterolateral to the fenestra cochleae. It is nearly circular in shape, with a length to width ratio (stapedial ratio of Segall 1970) of 1.2, similar to that of other palaeothentids (*Acdestis maddeni* has a stapedial ratio of 1.4; Goin et al. 2003). The shape of the fenestra vestibuli conforms tightly to the shape of the footplate of the stapes (e.g., Archibald 1979). As such, the footplate of
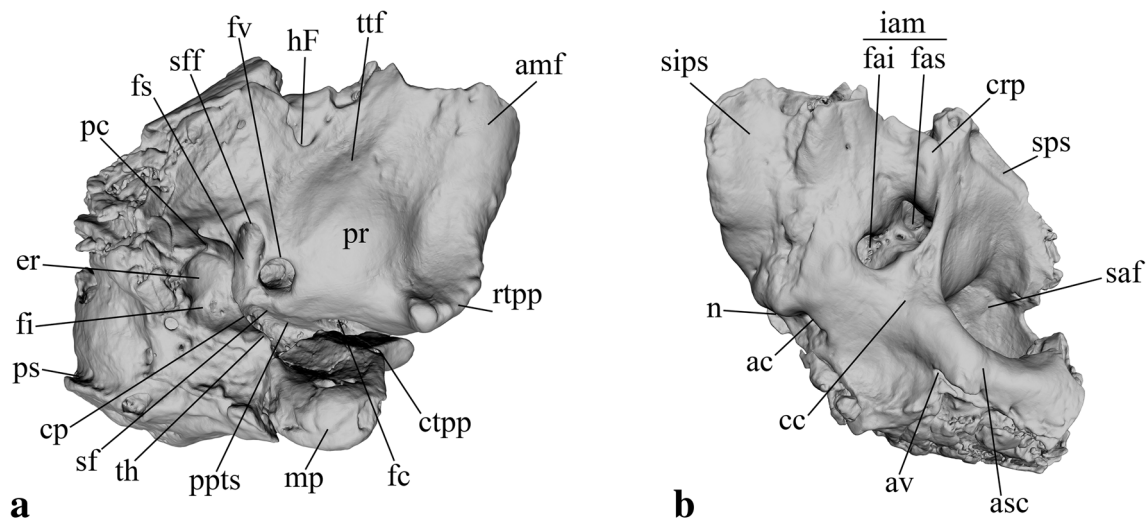
Fig. 5 *Palaeothentes lemoinei* (MPM-PV 3566). Model of the right petrosal based on 3D reconstructions from micro-CT data in tympanic (**a**) and cerebellar (**b**) views. *ac* aqueductus cochleae; *amf*, anteromedial flange; *asc*, anterior semicircular canal; *av* aqueductus vestibuli, *cc* crus commune, *cp* crista parotica, *crp* crista petrosa, *ctpp* caudal tympanic process, *er* epitympanic recess, *fai* inferior acoustic foramen, *fas* superior acoustic foramen, *fc* fenestra cochleae (=round window), *fi* fossa incudis, *fs* facial sulcus, *fv* fenestra vestibuli (=oval window), *hF* hiatus Fallopii, *iam* internal acoustic meatus, *mp* mastoid process, *n* notch for the jugular foramen, *pc* prootic canal, *ppts* postpromontorial tympanic sinus, *pr* promontorium, *ps* sulcus for the prootic sinus, *rtpp* rostral tympanic process of petrosal, *saf* subarcuate fossa, *sf* stapedial fossa, *sff* secondary facial foramen, *sips* sulcus for inferior petrosal sinus, *sps* sulcus for the superior petrosal sinus, *th* tympanohyal, *ttf* tensor tympani fossa

P. lemoinei would have been almost circular, as in most living marsupials and stem therians (Archibald 1979; Wible 1990, 2003; Rougier et al. 1998; except *Dromiciops*, some other australidelphians, and didelphimorphians with a stapedial ratio larger than 1.8; Segall 1970; Horovitz and Sánchez-Villagra 2003; Horovitz et al. 2008). The crista interfenestralis is wide and the fenestrae cochleae and the fenestra vestibuli are widely separate.

In tympanic view (Figs. 4a, 5a), the cavum supracochleare, which houses the geniculate ganglion, is covered by a bony bridge as in other metatherians (except juveniles and adult vombatids; Wible 1990; Rougier et al. 1998). The hiatus Fallopii, for the exit of the greater petrosal nerve (a branch of the facial nerve), is small and located in the tympanic side of the petrosal, as in *A. maddeni* (Goin et al. 2003) but differing from the dorsal position of *Caenolestes fuliginosus* (Sánchez-Villagra and Wible 2002). The secondary facial foramen, for the exit of the posterior branch of the facial nerve, is oval, slightly smaller than the fenestra vestibuli and opens posteroventrally into the facial sulcus. The secondary facial foramen and the fenestra vestibuli are adjacent. The facial sulcus is deep with parallel borders and oriented posteromedially towards the postpromontorial tympanic sinus. The postpromontorial tympanic sinus is narrower and even deeper than the facial sulcus. The stapedial fossa, for the attachment of the stapedius muscle, forms a small circular depression located in the postpromontorial tympanic sinus,

immediately posterior to the fenestra vestibuli. The stylomastoid notch is well defined between the tympanohyal and the caudal tympanic process. There is a notch on the medial border of the postpromontorial tympanic sinus forming the lateral border of the jugular foramen (Figs. 4a, 5a). As already mentioned, the caudal tympanic process is tall, resembling the condition of *Caenolestes* (Sánchez-Villagra and Wible 2002).

Lateral to the facial sulcus, there are two incompletely separated depressions: the epitympanic recess and the fossa incudis. The epitympanic recess, for the articulation of the malleus and incus, comprises a larger volume and is located more anterior than the fossa incudis. The fossa incudis, for the short process of the incus, is deeper and medially bordered by the crista parotica. The latter crest is short and increases its height medially. The crista parotica contacts the tympanohyal, a tall, robust process located posterior to the fenestra vestibuli. The tympanohyal (the ossified Reichert's cartilage) articulates with the stylohyal (the latter is not preserved in this specimen), joining the skull to the remaining elements of the hyoid apparatus (Wible 2003).

A small canal lateral to the facial sulcus is interpreted here as the prootic canal (Figs. 4a, 5a). The prootic canal would connect the prootic sinus with the lateral head vein (Wible 1990, 2003). The sulcus for the prootic sinus runs vertical on the mastoid process, in the squamosal view. The mastoid process (i.e., the region posteromedial to the

caudal tympanic process of the petrosal) is irregular in shape and pierced by several small foramina. The mastoid process would have been partially exposed in occipital view as in the living caenolestids and most living marsupials (Sánchez-Villagra and Wible 2002). Anterior to the promontorium and lateral to the anteromedial flange, the tympanic surface of the petrosal is pierced by several tiny foramina (Figs. 4a, 5a).

In cerebellar view (Figs. 4b, 5b), two main depressions are distinguished: the internal acoustic meatus and the subarcuate fossa. The internal acoustic meatus is deep and transversely wide. Inside the internal acoustic meatus, a broad crista transversa separates the superior acoustic foramen anterolaterally from the inferior acoustic foramen posteromedially (Figs. 4b, 5b). The crista transversa has a minute vascular foramen leading into the petrosal. The superior acoustic foramen is oval and splits into two small openings. The anterior aperture is the larger and corresponds to the canal for the facial nerve; it is directed ventrally, connecting the secondary facial foramen and hiatus Fallopii. The anterior border of the superior acoustic foramen has a shallow notch that would represent the passage of the facial nerve from the brain to the inner ear. The posterior aperture is partially hidden in cerebellar view by the posterolateral border of the internal acoustic meatus and would correspond to the aperture of the canal of the vestibular nerve from the membranous labyrinth (e.g., Wible 2003). The inferior acoustic foramen is round and has numerous small foramina of different size and random distribution and corresponds to the cribriform tract for passage of the fascicles of the cochlear nerve (Wible 1990, 2003). The lateral border of the internal acoustic meatus delimits a blunt crest oriented posteromedially to the anteromedial border of the subarcuate fossa. The crista petrosa is even lower than the already mentioned crest and is placed anterior to the internal acoustic meatus (Figs. 4b, 5b).

The subarcuate fossa is deep, with well-defined borders, as in most metatherians (except large-sized taxa with shallow fossae; Sánchez-Villagra 2002) and would house in life the cerebellar paraflocculus (e.g., MacIntyre 1972; Wible 1990, 2003). The aqueductus vestibuli is a small horizontal fissure, located on the medial side and at the level of the subarcuate fossa. This opening would transmit the endolymphatic duct and accompanying vein from the vestibular cavity (MacIntyre 1972; Wible 1990, 2003). The aqueductus cochleae (=cochlear canaliculus) is a small fissure opening medial to the internal acoustic meatus. The aqueductus cochleae would transmit the perilymphatic duct and accompanying vein from the inner ear cavity to the endocranium (MacIntyre 1972; Wible 1990, 2003).

The cerebellar view of the petrosal (Figs. 4b, 5b) shows two well-defined grooves that would correspond to the impression of the inferior and superior petrosal venous sinuses. The impression for the inferior petrosal sinus is on the anterior medial part of the petrosal, running antero-posteriorly. The inferior petrosal sinus would drain the blood into the internal jugular vein (e.g., Kay et al. 2008). In agreement with the soft tissue that the depression would convey, the sulcus for the inferior petrosal sinus in *P. lemoinei* extends to the level of the jugular notch. The sulcus for the superior petrosal sinus is narrower and located anterior to the subarcuate fossa.

Osseous inner ear. The osseous labyrinth consists of the cochlea, the vestibule, and the semicircular canals. The cochlea comprises the largest part of the osseous labyrinth and contains the cochlear duct.

In *P. lemoinei*, the cochlea coils with 1.9 turns, similar to *Caenolestes* sp. with 2 turns (Figs. 6d, 7d) The fenestra vestibuli is located ventral and slightly posterior to the lateral ampulla (Fig. 6a, b). The cochlear canaliculus, which transmits the aqueductus cochleae, is short and narrow at its base. It opens at the posterior border of the fenestra cochleae and extends medially. The fenestra cochleae is large and oval in shape. The vestibulum that contains the utricle and saccule is elongated (Fig. 6a, e). The anterior, posterior, and lateral semicircular canals (ASC, PSC, and LSC) are almost complete except the ASC, which is partially broken. The ASC forms the rim of the subarcuate fossa as seen in the cerebellar view of the petrosal (Fig. 5b). The PSC is vertical and forms the medial border of the subarcuate fossa; the LSC canal is in a perpendicular plane and forms its floor. The LSC is straight as seen in lateral view similar to *Caenolestes* (Fig. 6a, 7a), and differing from the undulate shape of some diprotodontians (*Phascolarctos* and *Vombatus*; Schmelzle et al. 2007) and *Dromiciops* (Fig. 7g). The angle between the ASC and PSC is 75° (measured on a plane parallel to the lateral semicircular canal and with the crus commune in the hinge; Fig. 6c). In *Caenolestes*, the angle is almost straight (Fig. 7c). The angle between the PSC and LSC is 90° in *P. lemoinei* (measured on a plane parallel to the ASC; Fig. 6a), similar to *Caenolestes*. The three semicircular canals of *P. lemoinei* and *Caenolestes* are nearly circular in shape (Fig. 6a, c, f). In *P. lemoinei,* the ratio between length and the width of the semicircular canals is nearly unity, consequently the canals are nearly circular. The length is defined as the distance between the mid-point of the arch of the canal that is the farthest away from the vestibulum to the vestibulum, while the width is the greatest dimension perpendicular to the length. In *P. lemoinei* the ASC length/width is 0.97—estimation after restoration—, the LSC length/width is 0.97, and the PSC length/width is 0.89. In *Caenolestes*, the ASC length/width is 0.96, the LSC length/width is 0.91, and the PSC length/width is 0.93.
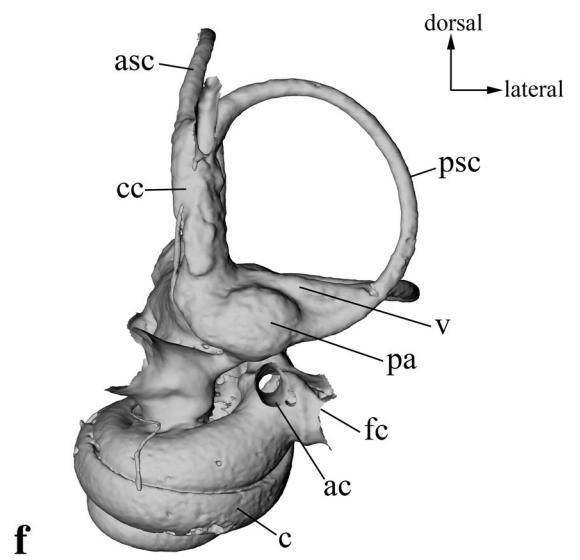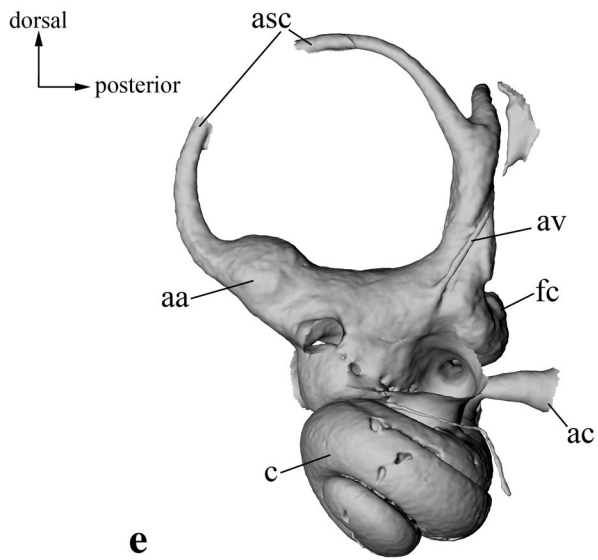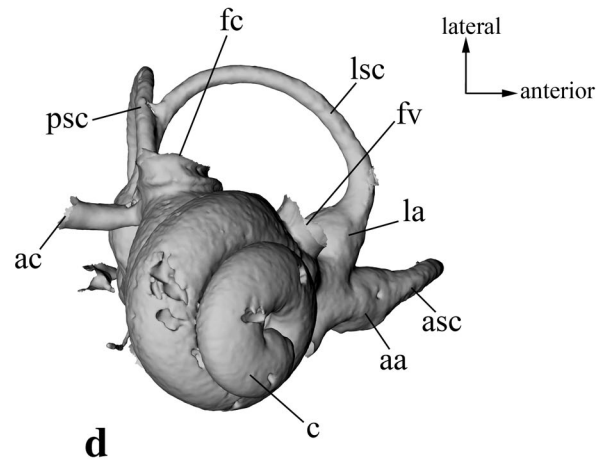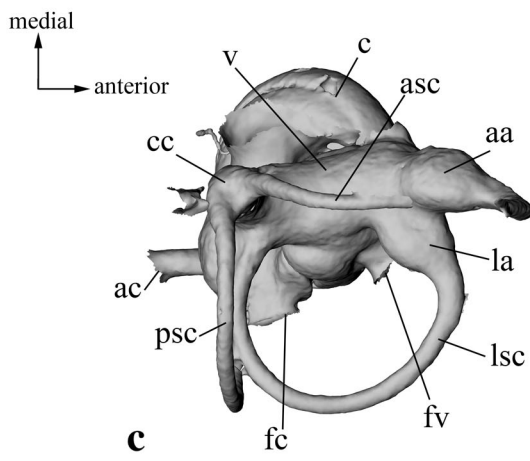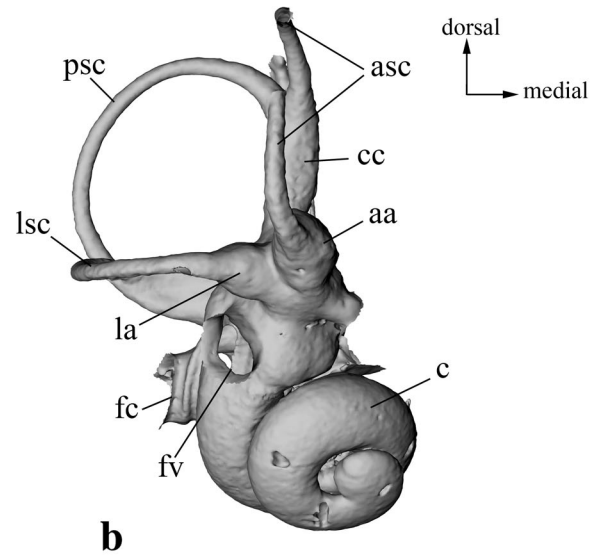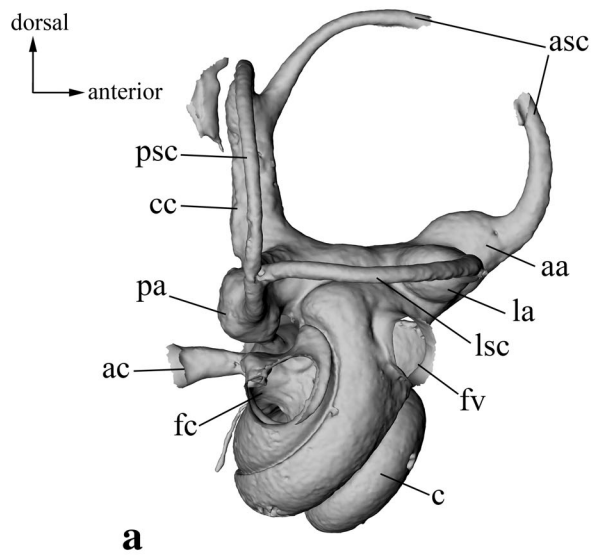
◄**Fig. 6** *Palaeothentes lemoinei* (MPM-PV 3566). Model of the osseous labyrinth based on 3D reconstructions from micro-CT data in lateral (**a**), anterior (**b**), dorsal (**c**), ventral (**d**), medial (**e**), and posterior (**f**) views. *aa* anterior ampulla, *ac* aqueductus cochleae, *asc* anterior semicircular canal, *asc* anterior semicircular canal, *av* aqueductus vestibuli, *c* cochlea, *cc* crus commune, *fc* fenestra cochleae (=round window), *fv* fenestra vestibuli (=oval window), *la* lateral ampulla, *lsc* lateral semicircular canal, *pa* posterior ampulla, *psc* posterior semicircular canal, *v* vestibule

The ASC slightly projects dorsally from the dorsal-most point of the PSC (Figs. 6b, 7b) in both paucituberculatans studied. The ratio between the extension of the dorsal projection of the ASC (i.e., distance between the dorsal-most point of the ASC to the dorsal-most point of the PSC)/height of PSC (measured in straight line from the LSC to the dorsal-most point of the PSC) is 0.20 in both taxa. The lateral extension of the LSC in *P. lemoinei* and *Caenolestes* is the same as the lateral extension of the PSC (Figs. 6c, 7c).

At the junction between the semicircular canals and the ventricule are the three ampullae (Fig. 6c). The anterior ampulla is on the anteroventral arm of the ASC and dorsolateral to the vestibulum, the lateral ampulla is on the anterior arm of the LSC and dorsolateral to the vestibulum, and the posterior ampulla is on the ventral arm of the PSC and ventromedial to the vestibulum. The crus commune is shorter than the length of the ASC (Fig. 6a) in *P. lemoinei* and *Caenolestes*. The posterior arm of the LSC and the ventral arm of the PSC join in a short canal and form a "second crus commune" (Schmelzle et al. 2007; Horovitz et al. 2008, 2009) in *P. lemoinei* (Fig. 6a) and in *Caenolestes* (Fig. 7c). The endocranial aperture of the aqueductus vestibuli is on the crus commune (Fig. 6e, f).

Dentary. The left dentary is almost complete except in lacking the condylar process (Fig. 8a–c), whereas the right dentary is represented by only the posterior portion (Fig. 8d–g). The horizontal ramus is deep, especially at the
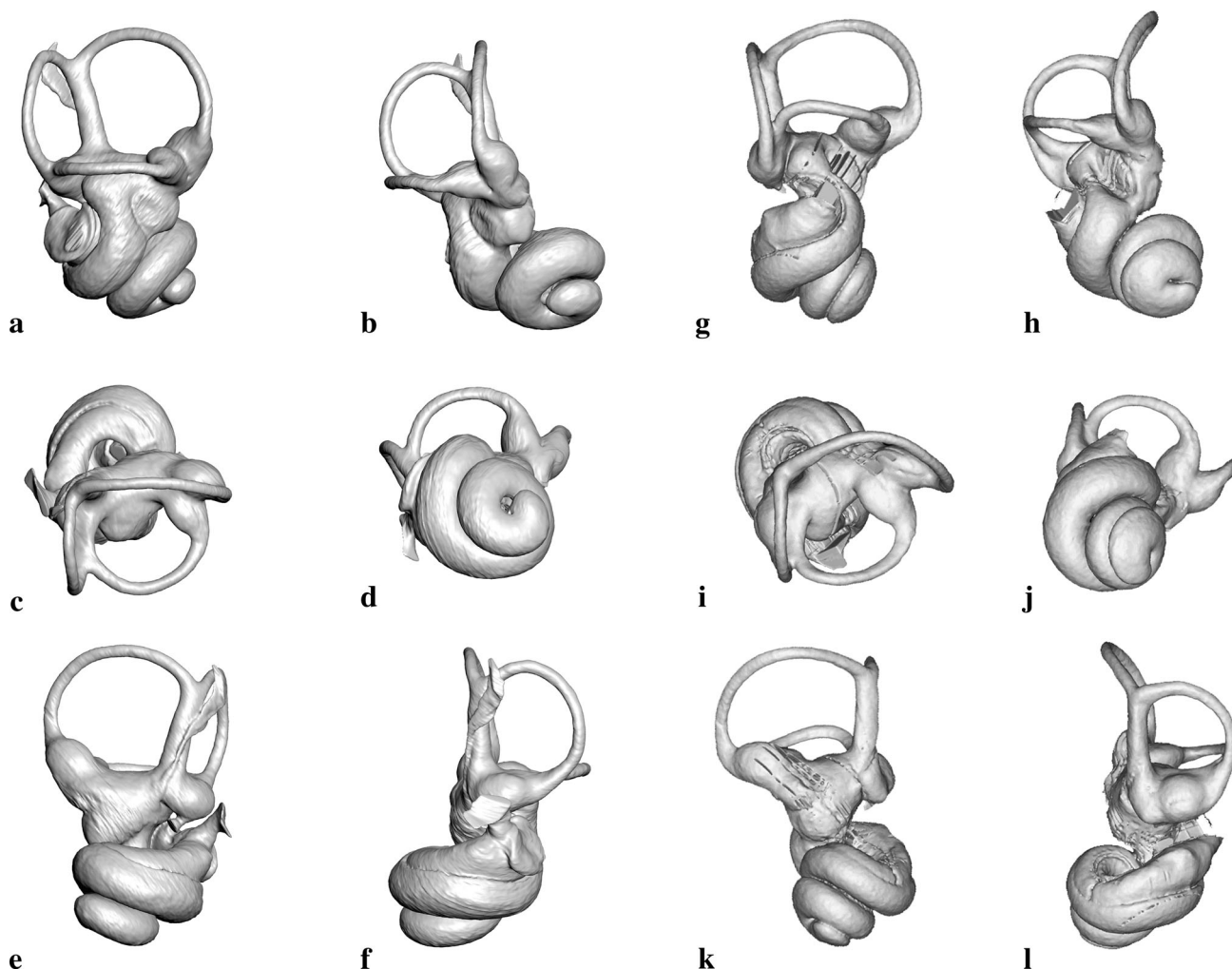

Fig. 7 Model of the osseous labyrinth based on 3D reconstructions from micro-CT data of *Caenolestes* sp. (**a–f**) and *Dromiciops gliroides* (**g–l**) in lateral (**a**, **g**), anterior (**b**, **h**), dorsal (**c**, **i**), ventral (**d**, **j**), medial (**e**, **j**), and posterior (**f**, **l**) views
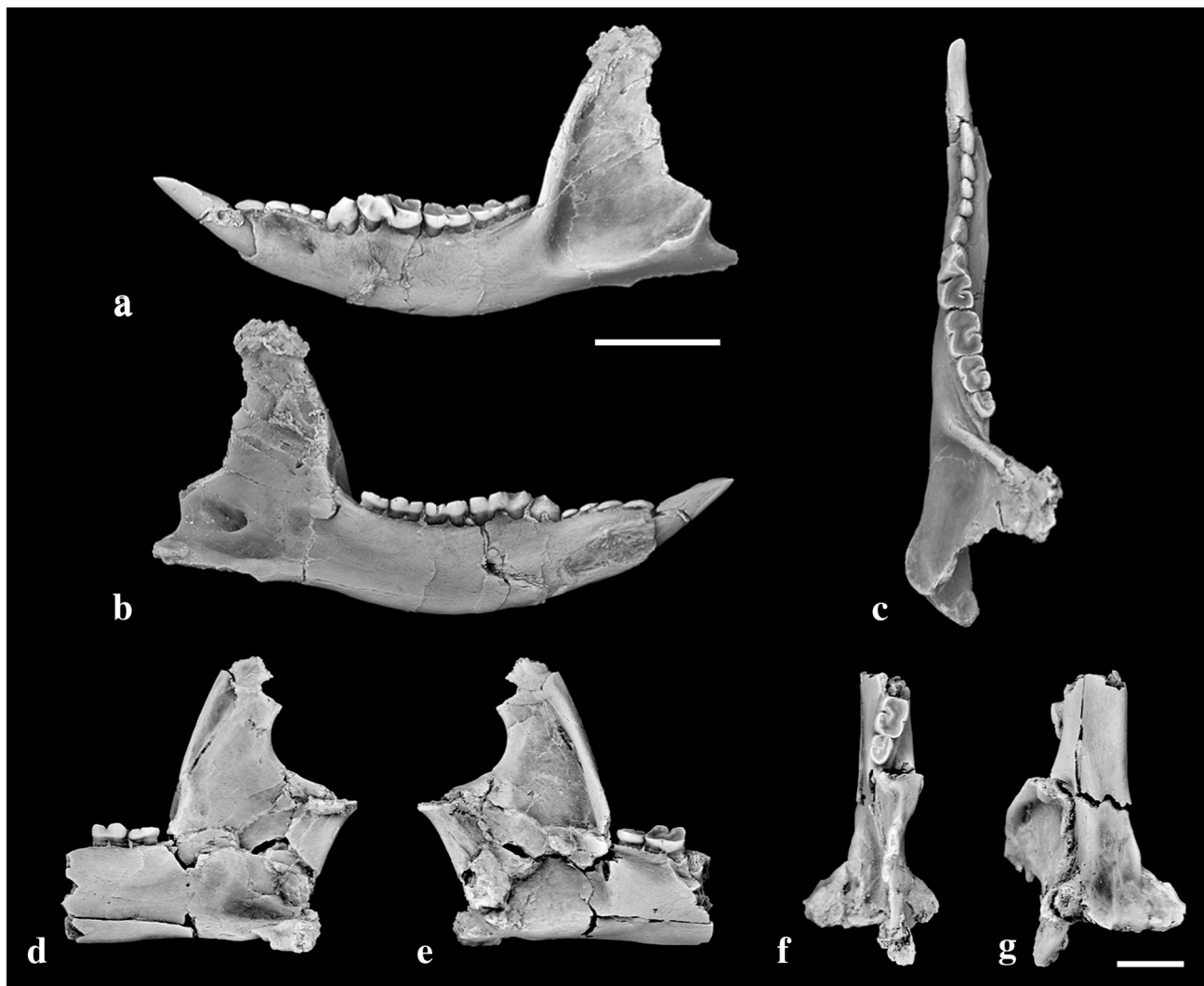
Fig. 8 *Palaeothentes lemoinei* (MPM-PV 3566). Left dentary in lateral (**a**), lingual (**b**), and occlusal (**c**) views. *Scale bar* 10 mm. Fragment of right dentary in lateral (**d**), lingual (**e**), occlusal (**f**), and ventral (**g**) views. *Scale bars* 5 mm

level of the molars (Table 1). An alveolus for the hypertrophied incisor occupies the entire anterior face of the dentary. The dorsal and ventral borders of the horizontal ramus are dorsally curved. There are two similar-sized mental foramina (Fig. 8a), as occurs generally in paucituberculatans (Marshall 1980): one is located at the level of the p2 and the other at the level of the trigonid of m1. The retromolar space, as seen in lateral view, is very short (i.e., the last molar is located very close to the anterior coronoid border). The lower teeth form a medially concave arch in occlusal view (Fig. 8c). The vertical process of the dentary is more than double the height of the horizontal process. The coronoid process is laminar and medially inflected. The anterior coronoid border rises at about 110° respect to the alveolar plane (Fig. 8a, e). Among living species, an obtuse angle is found in *Caenolestes* and *Rhyncholestes*,

while the angle is about 90° in *Lestoros* (Martin 2013). The masseteric fossa is broad and deep. There is no masseteric foramen. Among paucituberculatans, this opening was described for living and extinct taxa: *Caenolestes* following Osgood (1921) and *Abderites* following Abello and Rubilar-Rogers (2012).

In medial view (Fig. 8b), the symphysis extends posteriorly to the level of the anterior border of p3. The mandibular foramen opens posterior to the mid-point of the coronoid process.

The articular process is preserved on the right dentary. It is high and its position suggests that the condyle was located well above the alveolar level (Fig. 8d, e). The angular process is shelf-like (sensu Sánchez-Villagra and Smith 1997), and medially inflected, forming a small platform (Fig. 8f, g).

Dentition

The dentition in MPM-PV 3566 is in a very advanced stage of wear. Several structures are completely worn and the morphology is interpreted according to the general shape and the preserved bases of cusps. Detailed descriptions on the morphology of the dentition of *P. lemoinei* are in Marshall (1980), Bown and Fleagle (1993), and Abello (2007).

Upper dentition. The upper dental formula is: I3 C1 P3 M4 (Fig. 3a). There is no diastema between the incisors. The first (mesial) incisor (homologous to the I1 of other metatherians; Abello 2013) is the largest among the elements, slightly recumbent, with its tip extending ventrally about three times further than the posterior incisors. The I1 is heavily worn especially on its distal side. The second (I2) and third incisors (I3) are much smaller and placed distal and labial to I1. Both I1–I2 are similar in width, contrary to the condition in *Acdestis maddeni* in which the I2 is more laterally compressed (Goin et al. 2003). There is a short diastema between the last incisor and the canine, as in *A. maddeni* (Goin et al. 2003).

The canine is small, although larger than the following premolar, and labiolingually compressed (Fig. 3b). A small distema separates it from the P1.

The P1–P3 have two roots. A small diastema separates P1 from P2. P1 is the smallest premolar. P2 has a central high cusp and a much smaller posterior one. P3 is the largest premolar. Labially the P3 develops a high, subhorizontal and trenchant edge.

Molars decrease rapidly in size from M1 to M4. Because of wear, cusp features are not visible. The crowns are labiolingually wide compared to mesiodistal length. The M1 has a subquadrangular shape owing to a large metaconule. The posterior molars are subtriangular. The protocones protrude lingually, especially in M1 where there is also a perpendicular crest between the anterolingual and posterolingual faces of the protocone. Considering the labial contour of the molars, two main stylar cusps were present: StB and StC + D (according to the homologies established for other paucituberculatans; Abello 2007, 2013; Abello and Rubilar-Rogers 2012).

Lower dentition. There are six antemolar teeth in the dentary (Fig. 8a, c). The homologies of these teeth are difficult to establish. Ontogenetic evidence also makes the identification of the antemolar teeth tentative (Luckett and Hong 2000). It has been proposed that the teeth lost in the Palaeothentidae are the combination of i4, i5, c, p1 or p2 (Abello 2007, 2013). Here we follow previous authors in interpreting the hypertrophied lower incisor and its immediately distal tooth as i2 and i3, respectively (Hershkovitz 1995; Abello 2007). In MPM-PV 3566, the i2 is large and procumbent, as in other paucituberculatans and

closely related taxa (Marshall 1980; Abello 2007; Goin et al. 2009; Forasiepi et al. 2013). The four following teeth are small and simple in morphology. The teeth decrease in size from the first to the fourth element. In lateral view, these four teeth have collinear alveoli, with no lingual displacement at the second locus. The p3 is two-rooted, conspicuously larger than the preceding tooth and smaller than the m1. The molars decrease in size from m1 to m4, although the gradient is less steep than in *P. aratae*. In m1, the angle of the trigonid is obtuse (the paraconid has an anterior position), while in posterior molars the trigonid has an acute angle, that is, the paracristid is oriented more mesiodistally in m1 than in m4. The m1 trigonid and talonid are of similar length; in contrast, in *P. aratae* the m1 trigonid is proportionally longer than the talonid.

Postcranium

The postcranium is represented by several elements of the axial and appendicular skeleton. The axial skeleton is represented by 16 vertebrae belonging to the cervical, dorsal, sacral, and caudal regions (Fig. 9), and by fragmentary ribs. The appendicular skeleton is represented by a left humerus and ulna, both radii, the right pelvis, right femur, right astragalus, metapodials, and phalanxes. We concentrate here in the anatomy of the appendicular bones, as they provide useful characters for comparisons with other metatherians. Further descriptions on the morphology of the postcranium of *P. lemoinei* are to be found in Abello and Candela (2010) and Abello et al. (2012).

Humerus. The left humerus is complete except for some damage to the proximal part of the shaft (Fig. 10a, b). The head is displaced ninety degrees from its anatomical position. No parts of the shaft are missing, although it is anteroposteriorly compressed and a fracture distorts it from its original shape (the shaft in *Palaeothentes minutus* described by Abello and Candela 2010, Fig. 1, is more slender than in MPM-PV 3566).

The humerus is 76 % the length of the femur (Table 2). The humeral head is ovoid, dorsoventrally elongate and mediolaterally compressed with a length/width ratio of 1.36. The greater tuberosity is low relative to the projection of the humeral head, similar to *Lestoros*. A crest for the *m. teres major* is absent. The deltopectoral crest is broken and crushed proximally (Fig. 10a). Distally, the crest is raised and somewhat flattened suggesting that it formed a shelf (following Horovitz and Sánchez-Villagra 2003). However, the preserved parts are very unlike the condition in *Lestoros* in which the deltopectoral shelf is broad and flat. Our reconstruction of the length of the deltopectoral crest is about 15.9 mm, for a ratio of 42 % with the total humeral length. This crest does not extend as far distally on the shaft
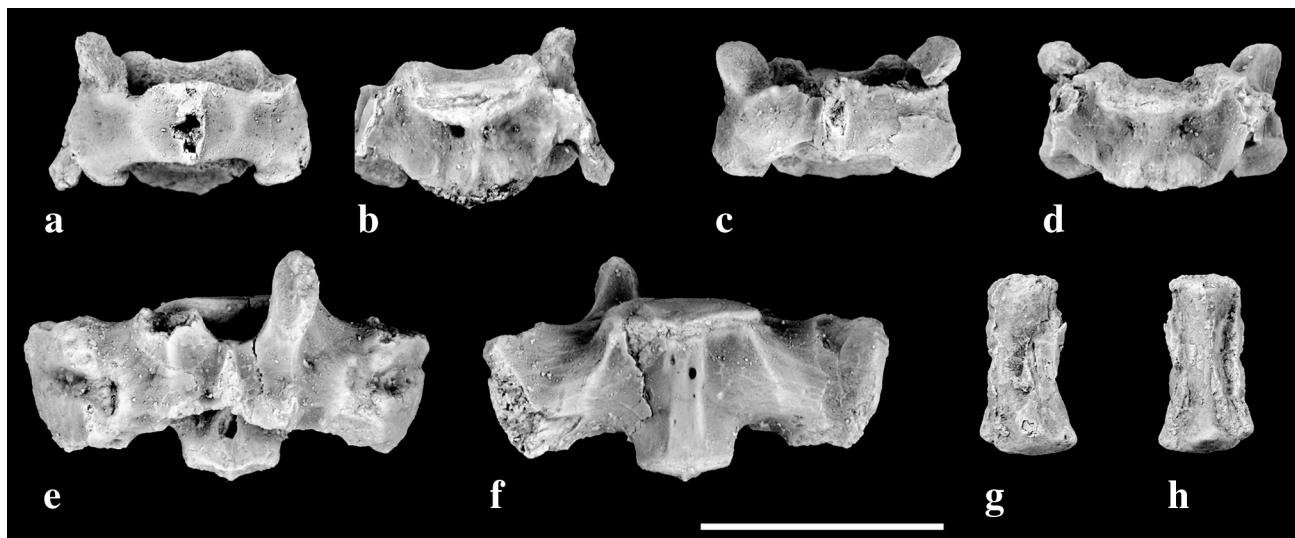
Fig. 9 *Palaeothentes lemoinei* (MPM-PV 3566). Two cervical vertebrae (**a–d**), the second sacral vertebra (**e**, **f**), one distal caudal vertebra (**g**, **h**) in dorsal and ventral views. *Scale bar* 10 mm

as in *Lestoros* and *Rhyncholestes*. The ectepicondylar crest is narrow (i.e., not salient) and long, representing 52 % of total the length of the bone (Fig. 10b). This differs from the short crest of *Lestoros* (ratio between ectepicondylar crest 4.8 mm/ total humeral length 16.25 mm = 29 %) and the narrower crest of *Rhyncholestes* and *Caenolestes* (Osgood 1921; Szalay and Sargis 2001). There is a large entepicondylar foramen. The supracondyloid crest partially covers the foramen, and the opening is not fully visible in anterior view, a difference from living caenolestids in which the foramen opens anteriorly (Abello and Candela 2010).

The medial epicondyle is even more reduced than in *Caenolestes* and *Rhyncholestes* (Osgood 1921; Szalay and Sargis 2001). The capitulum is ovoid and is less distally protruding compared to the trochlea. The coronoid fossa and radial fossa form a continuous depression. The trochlea is ovoid in distal view. As in *Lestoros*, the distal articular surface of *P. lemoinei* is extensive and bulges to form a 'pseudocapitulum' extending far medially to engulf most of the medial epicondyle. Sharp edges define the articular area in anterior and posterior view. In posterior view, the olecranon fossa is shifted laterally. It is deeper compared to *Lestoros*. In *P. minutus* the olecranon fossa is perforated (Abello and Candela 2010).

Ulna. The left ulna is well preserved except for lacking the distal part of the shaft and distal epiphysis (Fig. 10c, d). The olecranon process is relatively short and would comprise between 11 and 12 % the length of the bone (total length of the ulna estimated with the length of the radius; Table 2). This proportion of the olecranon is smaller than in *Caenolestes* (from Osgood's—1921—figures, the olecranon process comprises about 16 % of the total length of the ulna). The anconeal process is stout and sharp, as is the lateral

coronoid process. Together, the two processes define a deep trochlear notch. The trochlear notch index (following Szalay and Sargis 2001) is estimated to be 42. This value is similar to the value of 46 reported for *P. minutus* (Abello and Candela 2010) and the 44 reported for *Rhyncholestes* (Szalay and Sargis 2001). The medial portion of the ulnar proximal trochlear crest is widened and strongly sigmoid in shape and the ulnar cranial olecranon ridge is displaced medially in *P. lemoinei*, as in *Caenolestes* and *Rhyncholestes* (Szalay and Sargis 2001). The radial notch is offset laterally. The shaft of the ulna is mediolaterally compressed and curves anteriorly. Shallow grooves are developed on the lateral and medial sides of the shaft.

Radius. Both the right and left radius have been preserved, with the left element is in better condition (Fig. 10e, f). The radius is shorter than the ulna (about the 79 % of the total length of the ulna, Table 2) and anteroposteriorly compressed. The radial head is suboval in proximal view. The bicipital tuberosity is robust, oval, strongly posteriorly protruded and placed close to the radial head (Fig. 10f), as described for *P. minutus*. The radial shaft in *P. lemoinei* (Fig. 10e, f) is slightly curved, in contrast to the almost straight and slender shaft of *P. minutus* (Abello and Candela 2010). The styloid process is triangular and distally projected. In ventral view the distal epiphysis is shallowly concave and bears an oval and oblique facet for articulation with the scaphoid bone, which extends from the distal surface of the epiphysis to the lateral surface of the styloid process. The relation between the facets is gently curved (i.e., there is no trochlea).

Pelvis. The right pelvis is partially preserved, missing the anterior part of the illium and the pelvic symphysis

Fig. 10 *Palaeothentes lemoinei* (MPM-PV 3566). Left humerus in anterior (**a**) and posterior (**b**) views. Incomplete left ulna in medial (**c**) and lateral (**d**) views. Left radius in anterior (**e**) and posterior (**f**) views. Right pelvis in lateral (**g**) and medial (**h**) views. Right femur in anterior (**i**) and posterior (**j**) views. Proximal portion of fibula in medial view (**k**). *Scale bar* 10 mm

(Fig. 10g, h). The iliac wing is well developed and flattened anteriorly. The gluteal fossa is larger than the iliac fossa. The acetabular crest runs from the tubercle of the rectus femoris towards the iliac crest. The acetabular crest is robust and taller on the anterior part of the wing and separates the gluteal and iliac fossa. The tubercle of the rectus femoris is elongated and salient. The iliac crest forms the antero-dorsal border of the gluteal fossa. Because of the preservation, we cannot determine if the greater sciatic notch was deep (if the iliac crest abruptly joins the caudal dorso-border of the illium) or shallow as in *Caenolestes* (Osgood 1921). The ischial tubercle is distinct and the lesser sciatic notch is slightly deeper than in *Caenolestes* (Osgood 1921). The iliopubic eminence is

Table 2 Measurements of the postcranial elements (in mm)

Humerus	
Maximum length (restored)	36[a]
Humeral head dorsoventral length	7.67
Humeral head mediolateral breadth	5.63
Breadth of the proximal epiphysis	9.6[a]
Medial epicondyle length	4.65
Breadth of distal epiphysis (excluding medial epicondyle)	8.9
Entepicondylar crest	14.5 × 27.85
Ulna	
Maximum length (restored based on the radius)	41.4–45.8[a]
Olecranon process length	5.01
Olecranon process breadth	4.5
Radius	
Maximun length	36.35
Breadth of proximal epiphysis	3.86
Breadth of distal epiphysis	5
Femur	
Maximum length	49
Breadth of the proximal epiphysis	10.77
Breadth of the distal epiphysis	9.27
FCWI (femoral condyle width index, medial condyle width/lateral condyle width × 100	103
Fibula	
Breadth of the distal epiphysis	5.2
Astragalus	
Maximum anteroposterior length	6.65
Anteroposterior length of ectal facet	3
Medial breadth of ectal facet	4.9
Breadth of neck	2.5
Neck length	3.65
Autopodium	
Maximum length metacarpal a	9
Maximum length metacarpal b (no smaller than)	9.04[a]
Maximun length MCV	7
Maximun length metatarsal d	20
Maximum length metatarsal e (no smaller than)	20.05[a]
Maximum length phalanx (no smaller than)	7.7[a]

[a] The measurement is approximated

well defined as in *Caenolestes* and opossums, instead of being strongly developed as in macropodids among marsupials (Horovitz and Sánchez-Villagra 2003). The cranial portion of the acetabular area is somewhat distorted. This is a deep area with well-defined borders. Posteroventrally, the lunate surface is interrupted by a deep acetabular notch. The acetabular fossa was apparently round. The obturator foramen is incomplete but considering the borders preserved the opening was oval with a ventral projection as in *Caenolestes* (Osgood 1921).

Femur. The femoral head (Fig. 10i, j) is round in dorsal view, the greater trochanter projects proximally beyond the level of the femoral head, similar to living caenolestids (Osgood 1921; Szalay and Sargis 2001; Abello and Candela 2010). The trochanteric fossa is straight and long, as in other species of *Palaeothentes* (Abello and Candela 2010). The lesser trochanter is flat and triangular in shape similar to *Caenolestes* and *Rhyncholestes* (Osgood 1921; Szalay and Sargis 2001). There is a third trochanter on the lateral side of the femur, as in living and basal paucituberculatans (Szalay and Sargis 2001; Abello and Candela 2010) and marsupials from the Paleocene of Itaboraí (Szalay and Sargis 2001). The shaft is slightly dorsomedially compressed resulting from preservation, although it is clearly seen that the lateral and medial borders of the femur are almost parallel. On the posterior aspect, the medial condyle is slightly wider than the lateral one (FCWI, 103; Table 2). Wide medial condyles are present in *Rhyncholestes* (FCWI, 95; from Szalay and Sargis 2001) *and Caenolestes* (FCWI, 84; from Osgood 1921, Fig. 12). The intercondylar fossa is narrow and deep, and there is a shallow intercondylar notch.

Fibula. Only the proximal part of the fibula is preserved (Fig. 10k). The shaft is slender and according to the part preserved, it was slightly curved. Proximally it is somewhat expanded anteroposteriorly, although not as much as in didelphids (Szalay and Sargis 2001).

Astragalus. Only the right astragalus has been preserved (Fig. 11). In dorsal view (Fig. 11a), the dominant facets are the astragalofibular facet (AFi) and lateral astragalotibial facet (ATil). Both facets form a continuous surface with a narrow sulcus between forming a barely defined trochlea. The angle between the AFi and the ATil is approximately 180°, as in *Caenolestes*. The ATil is at about 90° from the medial astragalotibial facet (ATim) and there is a prominent medial trochlear crest between the two, as in *Caenolestes.* There is also a lateral trochlear crest on the lateral edge of the AFi. Whereas in *Caenolestes* the medial and lateral trochlear crests are almost parallel, in *P. lemoinei* they are at different angles. There is a projection of the ATim towards its medial border, absent in *Caenolestes* (Szalay 1994), and consequently the ATim is wider in the distal portion than in the proximal part, the opposite being the case in *Caenolestes* (Szalay 1994). Similarly, there is a distolateral expansion of the AFi, as is common among marsupials, including *Caenolestes* (Szalay, 1994), but absent in many eutherians (e.g., Salton and Szalay 2004, Fig. 3). The astragalar neck is clearly defined; it is as wide or slightly wider than the head, as in other metatherians (Horovitz 2000). A well-defined astragalotibial pit is located at the dorsal base of the neck. The astragonavicular facet (AN) extends on the ventromedial area of the head. In distal view, the AN is wider transversely than
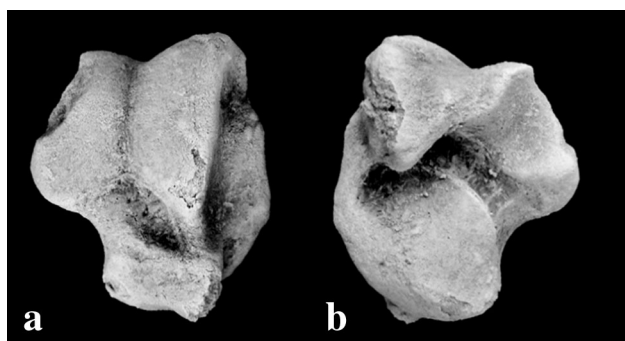
Fig. 11 *Palaeothentes lemoinei* (MPM-PV 3566). Right astragalus in dorsal (**a**) and plantar (**b**) views

dorsoventrally, as in *Caenolestes*. The AN is confluent with the sustentacular facet as in living caenolestids (Abello and Candela 2010).

In plantar view (Fig. 11b), the sustentacular facet is broad and slightly convex; it does not reach the medial edge of the astragalar neck. The AN is positioned anterior relative to the facets for the tibia and not medial to them as in at least some macropodoids among marsupials (Horovitz and Sánchez-Villagra 2003). The astragalar canal, which is present in *Yalkaparidon* and some dasyurids among marsupials (Szalay 1994; Horovitz and Sánchez-Villagra 2003, Beck et al. 2013), is absent in *P. lemoinei*. The longer dimension of the astragalocalcaneal facet (CaA) is orientated posteromedial to anterolaterally, as in *Caenolestes* and most marsupials. This facet is concave and extends to the posterior edge of the astragalus as in *Caenolestes*. The astragalar medial plantar tuberosity (ampt) is large although not visible in dorsal view.

Metapodials and phalanxes. The elements of the autopodium are disarticulated. The metacarpals (Fig. 12a–c) are shorter and more robust than the metatarsals. A short element with an oblique proximal articular facet and an asymmetrical trochlea (Fig. 12c) is interpreted as the fifth left metacarpal, based on comparisons with didelphids (see also Szalay and Sargis 2001). The two remaining are similar sized (Table 2). The symmetrical trochlea is well-preserved in one of them (Fig. 12a) and suggests that they could belong to mid-fingers (metacarpal second, third or forth). The metatarsals are very slender, long and with straight shaft (Fig. 12d, e). The proximal epiphysis is dorso-plantarly deep and narrow latero-medially. The trochlea is symmetrical with a well pronounced sagittal crest. One fragmentary phalanx (Fig. 12f) is interpreted from the anterior limb because the size and robustness is similar to the metacarpals. The shaft is broader proximally than distally.
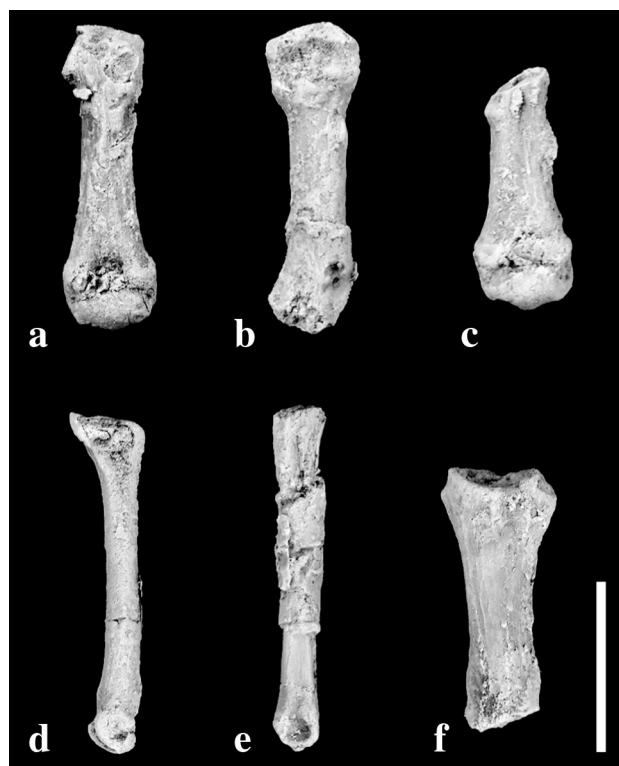

Fig. 12 *Palaeothentes lemoinei* (MPM-PV 3566). Metacarpals (**a**–**c**), metatarsals (**d**–**f**), and phalanx (**f**). *Scale bar* for **a**, **b**, **c**, **f** = 5 mm. *Scale bar* for **d**, **e** = 10 mm

Discussion

Skull and dentition

The dental morphology of palaeothentids is more derived than that of caenolestids (Goin et al. 2003), but the skull has more plesiomorphic traits, as shown by the study of MPM-PV 3566. The skull of *Palaeothentes lemoinei* is larger than extant caenolestids, with a shorter and broader snout, smaller palatal vacuities, proportionally narrower interorbital constriction, and a less globular and more triangular-shaped cranial vault in dorsal view. These features are shared with other Miocene paucituberculatans, such as the palaeothentids *Palaeothentes minutus*, *Acdestis oweni*, and *A. maddeni* (Sinclair 1906; Goin et al. 2003). In contrast, the dentition demonstrates unique features such as the reduction in number of the incisors, a p3/m1 shearing complex (although not to the extreme development of a plagiaulacoid m1 as in abderitids), and the molars with steeper size gradient from front to back (Marshall 1980; Bown and Fleagle 1993; Abello 2007).

The upper antemolar teeth are partially known in other palaeothentids (Abello 2013). MPM-PV 3566 clearly has seven upper antemolars as was inferred based on previous

specimens (*Acdestis maddeni* following Goin et al. 2003, and some specimens referred to *Palaeothentes minutus*, following Abello 2007) and whose homologies are considered to be I1–I3 C P1–P3 (Abello 2013). MPM-PV 3566 has six lower antemolar teeth as in other palaeothentids (Abello 2013), the homologies of which are not certain for all of them (for a discussion about this topic, see Abello 2013).

The limited but valuable knowledge provided by the few and incomplete known skulls of fossil paucituberculatans serves for comparisons with the new specimen of *P. lemoinei* (MPM-PV 3566). *P. lemoinei* differs from the *Acdestis maddeni* and *A. oweni* by a narrower interorbital constriction. For *Acdestis maddeni,* Goin et al. (2003) estimated an interorbital constriction width of 8.7 mm, ca. 1 mm wider than in MPM-PV 3566 although that skull of *Acdestis maddeni* (condylo-basal length 53.8 mm) is 10 mm smaller (85 % of MPM-PV 3566's size). Nasals are narrower in *P. lemoinei* than in *Acdestis oweni* and crests on the dorsal surface of the cranial vault are intermediate between *A. maddeni* with low crests and *A. oweni* with taller crests.

Until now, only *Acdestis maddeni* from the Middle Miocene (Laventan) of Bolivia (Goin et al. 2003) has provided information about the ear region of fossil paucituberculatans. *P. lemoinei* provides further details of this area, in particular the petrosal and osseous inner ear anatomy. Uniquely to date for a fossil South American marsupial, MPM-PV 3566 has been subject to a micro-CT scan.

In *P. lemoinei*, the cochlea has 1.9 turns similar to *Caenolestes* with 2 turns. This number is close to, but slightly outside the range commonly found in living marsupials in which the cochlea has between 2.4 and 3 turns (Sánchez-Villagra and Schmelzle 2007, e.g., *Dromiciops* with 2.5 turns: Fig. 7h). In contrast, stem marsupials have a less coiled cochlea, such as *Herpetotherium* with 1.6 turns (Horovitz et al. 2008), a Cretaceous metatherian from Montana with 1.5 turns (Meng and Fox 1995), and exceptionally some australidelphians such as *Vombatus ursinus* with 1.4 turns (Sánchez-Villagra and Schmelzle 2007) and *Notoryctes* with 1.6 turns (Ladevèze et al. 2008).

The osseous labyrinth of *P. lemoinei* exhibits a "second crus commune". Usually, the vestibulum is pierced by five openings that lead to (1) the crus commune, (2) the anterior arm of the ASC, (3) the anterior arm of the LSC, (4) the posterior arm of the LSC, and (5) the inferior arm of the PSC, as occurs in *Dromiciops* among the taxa studied here (Fig. 7a, g). However, in some marsupials, as *P. lemoinei*, and *Caenolestes* there are four openings by the common entrance of the posterior arm of the LSC and the inferior arm of the PSC through a "second crus commune" (Schmelzle et al. 2007). A "second crus commune" was described for *Herpetotherium*, *Mimoperadectes*,

Diprotodon, *Thylacoleo*, and living marsupials including didelphids, dasyurids, and paramelids (Sánchez-Villagra and Schmelzle 2007; Schmelzle et al. 2007; Horovitz et al. 2008, 2009; Alloing-Séguier et al. 2013) and is reportedly plesiomorphic for Mammaliaformes (Ruf et al. 2013). Its finding in *P. lemoinei* further suggests a broader distribution of this character among metatherians.

P. lemoinei is a medium sized taxon (about 350 g; Abello et al. 2012), similar in body mass to *Pseudocheirus canescens* among extant marsupials (Smith et al. 2003). It has been demonstrated that the shape of the osseous labyrinth has a strong allometric relationship (Alloing-Séguier et al. 2013) and comparisons with the available data suggest that *P. lemoinei* is no exception. The labyrinths in larger marsupials have (1) the ASC and PSC proportionally larger and the LSC proportionally less developed, (2) the cochlea relatively smaller and laterally oriented, and (3) a longer crus commune (Alloing-Séguier et al. 2013). In *P. lemoinei*, in accordance with its body size, no allometrically unexpected differences have been detected in the size of the semicircular canals; the spiral of the cochlea represents a large portion of the osseous labyrinth, and ASC and PSC bifurcate distantly from their most extent dorsal border, resulting in a relative short crus commune (in clear contrast, the ASC and PSC bifurcate at the level of the dorsal border of the semicircular canals in *Diprotodon*, resulting in a long crus commune; Alloing-Séguier et al. 2013).

The shape of the semicircular canals reflects the membranous ducts within. The semicircular canals of the vestibular system are involved in the perception of changes in the rotational acceleration of the head (Malinzak et al. 2012). Only two studies have examined the correspondence between the size and shape of the semicircular canals and locomotion specifically in marsupials, and in particular in diprotodontians (Schmelzle et al. 2007; Alloing-Séguier et al. 2013). The postcranial anatomy of *P. lemoinei* suggests that this species was an agile terrestrial marsupial (Abello and Candela 2010; Abello et al. 2012; see also below), and, therefore, the morphology of the semicircular canals may correlate with a precise coordination.

In *P. lemoinei* as in *Caenolestes*, the ASC projects slightly dorsally from the dorsal-most point of the PSC (Fig. 6a) and the ratio between the extension of the dorsal projection of the ASC/height of PSC is 0.20. This estimation is in the range of quadruped species (see Schmelzle et al. 2007 for a discussion of this character and comparisons between marsupials). In diprotodontians bipedal species with erected posture (i.e., *Bettongia*, *Dorcopsis*, and *Macropus*) this ratio is larger than 0.42 (Schmelzle et al. 2007).

In *P. lemoinei*, the extension of the LSC is the same as the lateral extension of the PSC (Fig. 6c), as it is in

Caenolestes (Fig. 7c). This condition has been found in species with precise coordination, such as the arboreal taxa (e.g., *Dromiciops*; Fig. 7i), or in taxa that use a smaller and more complex substrate (i.e., smaller and more exact steps; Schmelzle et al. 2007). This character may be correlated to locomotion; however, it has also been found to vary intraspecifically and it is strongly influenced by body size and phylogeny (Schmelzle et al. 2007; Alloing-Séguier et al. 2013). We report a similar length of the LSC and PSC in both paucituberculatans, closer phylogenetically and of similar locomotion.

Postcranium

Only two partial skeletons of fossil paucituberculatans are known to date, those of *P. minutus* (MACN 5619–5639) and *P. lemoinei* (MPM-PV 3494) (Abello and Candela 2010; Abello et al. 2012). The new specimen (MPM-PV 3566) has provided information about the anatomy of the radius, femur, and metapodials of *P. lemoinei* and additional information about the pelvic girdle.

The paleobiology of *Palaeothentes*, including the locomotion, was analysed by Abello and Candela (2010) and Abello et al. (2012) on the basis of postcranial remains of *P. minutus* and *P. lemoinei*. These studies suggested that *Palaeothentes* would have been an agile cursorial dweller with leaping ability, similar to *Caenolestes*, *Lestoros,* and the didelphid *Metachirus* (Abello and Candela 2010; Abello et al. 2012). The study of MPM-PV 3566 supports this conclusion. Considering the characters previously analysed that are informative for paleobiological reconstructions (Szalay and Sargis 2001; Abello and Candela 2010; Abello et al. 2012), the new specimen of *P. lemonei* has the following in the forelimb: (1) humerus with a relatively short deltopectoral crest, (2) short ectepicondylar crest, (3) poorly protruding medial epicondyle, (4) high and deep humeral trochlea, and its correspondence in the ulna with a deep and close trochlear notch, with protruding borders, (5) the ulna with short olecranon process, (6) suboval radial head, and (7) large and protruding bicipital tuberosity. Those features are present in living terrestrial marsupials (e.g., caenolestids as well as *Metachirus*, the latter an agile, cursorial-to-saltatorial opossum), supporting the paleoecological interpretation of *P. lemoinei* as a mainly terrestrial animal (Abello and Candela 2010). Differing from the described morphology of *P. minutus* (Abello and Candela 2010; Abello et al. 2012), MPM-PV 3566 has a curved ulnar and radial shaft and a wider radial shaft. This could represent intraspecific variation, although the possibility of taphonomic distortion affecting the real shape of the bone cannot be ruled out. In the hindlimb, (1) the pelvis has a deep acetabulum with protruding borders, (2) the femur has a greater trochanter projecting beyond the level of the femoral head, and (3) a reduced lesser trochanter, and (4) a third trochanter, (5) lateral condyle slightly narrower than medial one, (6) astragalus with a strong angle between the ATil and ATim facets, and (6) a slightly grooved trochlea. The last feature is unique among the known fossil metatherians from South America. No grooved trochlea has been found in the Sparassodonta (Argot 2004; Forasiepi 2009) a group represented by terrestrial species, even though some species achieved a certain degree of cursoriality (Argot 2004; Ercoli and Prevosti 2012). The presence of a trochlear groove and lateral and medial crests surrounding the ATil and AFi indicates some degree of restriction of mediolateral mobility of the lower ankle joint and facilitation of stability in flexion and extension (Szalay 1994, and references therein). As reviewed and studied in a wide range of mammals by Szalay and other authors (e.g., Szalay 1994; Nakatsukasa et al. 1997; Szalay and Sargis 2001), the shape and configuration of the astragalus reflects not only phylogenetic history but also the direction and distribution of incurred loads from the crus.

Conclusion

Compared to that of living caenolestids, the skull of *Palaeothentes lemoinei* has more plesiomorphic traits in the face, palate, and cranial vault than living paucituberculatans; whereas the dental morphology is more derived. The analysis of the osseous inner ear revealed a cochlea with 1.9 turns, the presence of a second "crus commune", an ASC projecting slightly dorsally from the dorsal-most point of the PSC, and an LSC and PSC projecting laterally up to the same level.

The specimen provides new information about the anatomy of the radius, pelvic girdle, femur, and metapodials. Previous studies have demonstrated that *P. lemoinei* was an agile cursorial dweller and we supported this inference with the new data.

References

Abello, M. A. (2007). Sistemática y bioestratigrafía de los Paucituberculata (Mammalia, Marsupialia) del Cenozoico de América

del Sur. Unpublished PhD thesis, Universidad Nacional de La Plata, 381 pp.

Abello, M. A. (2013). Analysis of dental homologies and phylogeny of Paucituberculata (Mammalia: Marsupialia). *Biological Journal of the Linnean Society, 109*, 441–465.

Abello, M. A., & Candela, A. M. (2010). Postcranial skeleton of the Miocene marsupial *Palaeothentes* (Paucituberculata, Palaeothentidae): Paleobiology and phylogeny. *Journal of Vertebrate Paleontology, 30*, 1515–1527.

Abello, M. A., Ortiz-Jaureguizar, E., & Candela, A. M. (2012). Paleoecology of the Paucituberculata and Microbiotheria (Mammalia, Marsupialia) from the late early Miocene of Patagonia. In R. F. Kay, S. Vizcaíno, & S. Bargo (Eds.), Paleobiology in Patagonia. Reconstructing a high-latitude paleocommunity in the early Miocene climatic optimum (pp. 156–172). Cambridge: Cambridge University Press.

Abello, M. A., & Rubilar-Rogers, D. (2012). Revisión del género *Abderites* Ameghino, 1887 (Marsupialia, Paucituberculata). *Ameghiniana, 49*, 164–184.

Alloing-Séguier, L., Sánchez-Villagra, M. R., Lee, M. S. Y., & Lebrun, R. (2013). The bony labyrinth in diprotodontian marsupial mammals: Diversity in extant and extinct forms and relationships with size and phylogeny. *Journal of Mammalian Evolution, 20*, 191–198.

Ameghino, F. (1887). Enumeración sistemática de las especies de mamíferos fósiles coleccionados por Carlos Ameghino en los terrenos eocenos de la Patagonia austral y depositados en el Museo de La Plata. *Boletín Museo de La Plata, 1*, 1–26.

Ameghino, F. (1894). Enumération synoptique des espéces de mammifères fossiles des formations éocènes de Patagonie. *Boletín de la Academia Nacional de Ciencias de Córdoba, 13*, 259–452.

Archibald, J. D. (1979). Oldest known eutherian stapes and a marsupial petrosal bone from the Late Cretaceous of North America. *Nature, 281*, 669–670.

Argot, C. (2004). Evolution of South American mammalian predators (Borhyaenoidea): Anatomical and palaeobiological implications. *Zoological Journal of Linnean Society, 140*, 487–521.

Asher, R. J., Horovitz, I., & Sánchez-Villagra, M. R. (2004). First combined cladistic analysis of marsupial mammal interrelationships. *Molecular Phylogenetics and Evolution, 33*, 240–250.

Baker, M. L., Wares, J. P., Harrison, G. A., & Miller, R. D. (2004). Relationships among the families and orders of marsupials and the major mammalian lineages based on recombination activating gene-1. *Journal of Mammalian Evolution, 11*, 1–16.

Beck, R. M. D. (2008). A dated phylogeny of marsupials using a molecular supermatrix and multiple fossil constraints. *Journal of Mammalogy, 89*, 175–189.

Beck, R. M. D., Godthelp, H., Weisbecker, V., Archer, M., & Hand, S. J. (2008). Australia's oldest marsupial fossils and their biogeographical implications. *PLoS One, 3*(3), e1858. doi:10.1371/journal.pone.0001858.

Beck, R. M. D., Travouillon, K. J., Aplin, K. P., Godthelp, H., & Archer, M. (2013). The osteology and systematics of the enigmatic Australian Oligo-Miocene metatherian *Yalkaparidon* (Yalkaparidontidae; Yalkaparidontia; ?Australidelphia; Marsupialia). *Journal of Mammalian Evolution*. doi:10.1007/s10914-013-9236-3.

Bown, T. M., & Fleagle, J. G. (1993). Systematics, biostratigraphy, and dental evolution of the Palaeothentidae, later Oligocene to early-middle Miocene (Deseadan-Santacrucian) caenolestoid marsupials of South America. *Journal of Paleontology, 67*, 1–76.

Dederer, P. H. (1909). Comparison of *Caenolestes* with Polyprotodonta and Diprotodonta. *The American Naturalist, 43*, 614–618.

Dumont, E. R., & Bown, T. M. (1997). New caenolestoid marsupials. In R. F. Kay, R. H. Madden, R. H. Cifelli, & J. J. Flynn (Eds.) Vertebrate paleontology in the Neotropics. The Miocene fauna of La Venta (pp. 207–212). Washington, DC: Smithsonian Institution Press.

Ercoli, M. D., & Prevosti, F. J. (2012). Estimación de masa de las especies de Sparassodonta (Metatheria, Mammalia) de la Edad Santacrucense (Mioceno Temprano) a partir de tamañnos de centroide de elementos apendiculares: inferencias paleoecológicas. *Ameghiniana, 48*, 462–479.

Forasiepi, A. M. (2009). Osteology of *Arctodictis sinclairi* (Mammalia, Metatheria, Sparassodonta) and phylogeny of Cenozoic metatherian carnivores from South America. *Monografías del Museo Argentino de Ciencias Naturales, 6*, 1–174.

Forasiepi, A. M., Goin, F. J. Abello, M. A., & Cerdeño, E. (2013). A unique, late Oligocene shrew-like marsupial from western Argentina and the evolution of dental morphology marsupial. Journal of Systematic Palaeontology. doi:10.1080/14772019.2013.799611.

Goin, F. J., Abello, M. A., & Chornogubsky, L. (2010). Middle Tertiary marsupials from central Patagonia (early Oligocene of Gran Barranca): Understanding South America's Grande Coupure. In R. H. Madden, A. A. Carlini, M. G. Vucetich, & R. F. Kay (Eds.), *The Paleontology of Gran Barranca: Evolution and Environmental Change through the Middle Cenozoic of Patagonia* (pp. 69–105). Cambridge: Cambridge University Press.

Goin, F. J., Candela, A. M., Abello, M. A., & Oliveira, E. V. (2009). Earliest South American paucituberculatans and their significance in the understanding of 'pseudodiprotodont' marsupial radiations. *Zoological Journal of the Linnean Society, 155*, 867–884.

Goin, F. J., Sánchez-Villagra, M. R., Abello, M. A., & Kay, R. F. (2007). A new generalized paucituberculatan marsupial from the Oligocene of Bolivia and the origin of 'shrew-like' opossums. *Palaeontology, 50*, 1267–1276.

Goin, F. J., Sánchez-Villagra, M. R., Kay, R. F., Anaya-Daza, F., & Takai, M. (2003). New palaeothentid marsupial from the middle Miocene of Bolivia. *Palaeontology, 46*, 307–315.

Graf, W., & Klam, F. (2006). Le système vestibulaire: anatomie fonctionnelle et comparée, évolution et développement. *Comptes Rendus Palevol, 5*, 637–655.

Hershkovitz, P. (1995). The staggered marsupial third lower incisor: Hallmark of cohort Didelphimorphia, and description of a new genus and species with staggered i3 from the Albian (Lower Cretaceous) of Texas. *Bonner Zoologische Beitrage, 45*, 153–169.

Hershkovitz, P. (1997). Composition of the family Didelphidae Gray, 1821 (Didelphoidea: Marsupialia), with a review of the morphology and behavior of the included four-eyed pouched opossums of the genus *Philander* Tiedemann, 1808. *Fieldiana Zoology, 86*, 1–103.

Horovitz, I. (2000). The tarsus of *Ukhaatherium nessovi* (Eutheria, Mammalia) from the Late Cretaceous of Mongolia: An appraisal of the evolution of the ankle in basal therians. *Journal of Vertebrate Paleontology, 20*, 547–560.

Horovitz, I., Ladeveze, S., Argot, C., Macrini, T. E., Martin, T., et al. (2008). The anatomy of *Herpetotherium* cf. *fugax* Cope, 1873, a metatherian from the Oligocene of North America. *Palaeontographica Abteilung A, 284*, 109–141.

Horovitz, I., Martin, T., Bloch, J., Ladevèze, S., Kurz, C., & Sánchez-Villagra, M. R. (2009). Cranial anatomy of the earliest marsupials and the origin of opossums. *PLoS One, 4*(12), e8278. doi:10.1371/journal.pone.0008278.

Horovitz, I., & Sánchez-Villagra, M. R. (2003). A morphological analysis of marsupial mammal higher-level phylogeny relationships. *Cladistics, 19*, 181–212.

Illiger, C. (1811). *Prodromus Systematis Mammalian et Avium Additis Terminus Zoographicis Utriudque Classis*. Berlin: C. Salfed.

Kay, R. F., Ross, J., & Simons, E. L. (2008). The basicranial anatomy of African Eocene/Oligocene anthropoids. Are there any clues for platyrrhine origins? In J. G. Fleagle, & C. G. Gilbert (Eds.), Elwyn L. Simons: A search for origins (pp. 125–158). New York: Springer.

Koyabu, D. B., Maier, W., & Sánchez-Villagra, M. R. (2012). Paleontological and developmental evidence resolve the homology and dual embryonic origin of a mammalian skull bone, the interparietal. *Proceedings of the National Academy of Sciences USA, 109*, 14075–14080.

Ladevèze, S., Asher, R. J., & Sánchez-Villagra, M. R. (2008). Petrosal anatomy in the fossil mammal *Necrolestes*: Evidence for metatherian affinities and comparisons with the extant marsupial mole. *Journal of Anatomy, 213*, 686–697.

Losch, C., Losch, P., Kurz, R., & Kühn, T. (1999). Cinema 4D. Friedrichsdorf: Maxon Computer.

Luckett, W. P., & Hong, N. (2000). Ontogenetic evidence for dental homologies and premolar replacement in fossil and extant caenolestids (Marsupialia). *Journal of Mammalian Evolution, 7*, 109–127.

MacIntyre, G. T. (1972). The trisulcate petrosal pattern of mammals. In T. Dobzhansky, M. K. Hecht, & W. C. Steere (Eds.), *Evolutionary Biology* (Vol. 6, pp. 275–303). New York: Appleton-Century-Crofts.

Malinzak, M. D., Kay, R. F., & Hullar, T. E. (2012). Locomotor head movements and semicircular canal morphology in primates. *Proceedings of the National Academy of Sciences USA, 109*(44), 17914–17919.

Marshall, L. G. (1980). Systematics of the South American marsupial family Caenolestidae. *Fieldiana Geology, 5*, 1–145.

Marshall, L. G. (1990). Fossil Marsupialia from the type Friasian Land Mammal Age (Miocene), Alto Rio Cisnes, Aisen, Chile. *Revista Geológica de Chile, 17*, 19–55.

Marshall, L. G., & de Muizon C. (1995). The skull. In L. G. Marshall, C. de Muizon, & D. Sigogneau-Russell (Eds.), *Pucadelphys andinus* (Marsupialia, Mammalia) from the early Paleocene of Bolivia, Part II. Mémoires du Muséum National d'Histoire Naturelle, vol. 165 (pp. 21–90).

Martin, G. M. (2013). Intraspecific variability in *Lestoros inca* (Paucituberculata, Caenolestidae), with reports on dental anomalies and eruption pattern. *Journal of Mammalogy, 94*, 601–617.

Meng, F., & Fox, R. C. (1995). Osseous inner ear structures and hearing in early marsupial and placentals. *Zoological Journal of the Linnean Society, 115*, 47–71.

Meredith, R. W., Janecka, J. E., Gatesy, J., Ryder, O. A., Fisher, C. A., Teeling, E. C., et al. (2011). Impacts of the Cretaceous terrestrial revolution and KPg extinction on mammal diversification. *Science, 334*, 521–524.

Meredith, R. W., Westerman, M., Case, J. A., & Springer, M. S. (2008). A phylogeny and timescale for marsupial evolution based on sequences for five nuclear genes. *Journal of Mammalian Evolution, 15*, 1–36.

Meredith, R. W., Westerman, M., & Springer, M. S. (2009). A phylogeny of Diprotodontia (Marsupialia) based on sequences for five nuclear genes. *Molecular Phylogenetics and Evolution, 51*, 554–571.

Nakatsukasa, M., Takai, M., & Setoguchi, T. (1997). Functional morphology of the postcranium and locomotor behavior of *Neosaimiri fieldsi*, a *Saimiri*-like Middle Miocene platyrrhine. *American Journal of Physical Anthropology, 102*, 515–544.

Nilsson, M. A., Arnason, U., Spencer, P. B. S., & Janke, A. (2004). Marsupial relationships and a timeline for marsupial radiation in South Gondwana. *Gene, 340*, 189–196.

Nilsson, M. A., Churakov, G., Sommer, M., Tran, N. V., Zemann, A., Brosius, J., & Schmitz, J. (2010). Tracking marsupial evolution using archaic genomic retroposon insertions. *PLoS Biology*, *8*, e1000436. doi:10.1371/journal.pbio.1000436.

Ojala-Barbour, R., Pinto, C. M., Brito, J., Albuja, L., Lee, T. E., & Patterson, B. D. (2013). A new species of shrew-opossum (Paucituberculata: Caenolestidae) with a phylogeny of extant caenolestids. *Journal of Mammalogy, 94*, 967–982.

Osgood, W. H. (1921). A monographic study of the American marsupial, *Caenolestes*. Field Museum of Natural History, Zoological Series, vol. 14 (pp. 1–162).

Osgood, W. H. (1924). Review of living caenolestids with description of a new genus from Chile. Field Museum Natural History Publications Zoological Series, vol. 14, pp. 165–173.

Patterson, B. D., & Gallardo, M. H. (1987). Rhyncholestes raphanurus. *Mammalian Species, 286*, 1–5.

Rougier, G. W., Wible, J. R., & Novacek, M. J. (1998). Implications of *Deltatheridium* specimens for early marsupial history. *Nature, 396*, 459–463.

Ruf, I., Luo, Z.-X., & Martin, T. (2013). Re-investigation of the basicranium of *Haldanodon exspectatus* (Mammaliaformes, Docodonta). *Journal of Vertebrate Paleontology, 33*, 382–400.

Salton, J. A., & Szalay, F. S. (2004). The tarsal complex of Afro-malagasy Tenrecoidea: A search for phylogenetically meaningful characters. *Journal of Mammalian Evolution, 11*, 73–104.

Sánchez-Villagra, M. R. (2001). The phylogenetic relationships of argyrolagid marsupials. *Zoological Journal of the Linnean Society, 131*, 481–496.

Sánchez-Villagra, M. R. (2002). The cerebellar paraflocculus and the subarcuate fossa in *Monodelphis domestica* and other marsupial mammals: The ontogeny and phylogeny of a brain–skull interaction. *Acta Theriologica, 47*, 1–14.

Sánchez-Villagra, M. R., & Schmelzle, T. (2007). Anatomy and development of the bony inner ear in the woolly opossum, *Caluromys philander* (Didelphimorphia, Marsupialia). *Mastozoología Neotropical, 14*(1), 53–60.

Sánchez-Villagra, M. R., & Smith, K. K. (1997). Diversity and evolution of the marsupial mandibular angular process. *Journal of Mammalian Evolution, 4*, 119–144.

Sánchez-Villagra, M. R., & Wible, J. R. (2002). Patterns of evolutionary transformation in the petrosal bone and some basicranial features in marsupial mammals, with special reference to didelphids. *Journal of Zoological Systematics and Evolutionary Research, 40*, 26–45.

Schaller, O. (1992). *Illustrated veterinary anatomical nomenclature*. Stuttgart: Ferdinand Enke Verlag.

Schmelzle, T., Sánchez-Villagra, M. R., & Maier, W. (2007). Vestibular labyrinth evolution in diprotodontian marsupial mammals. *Mammal Study, 32*, 83–97.

Segall, W. (1970). Morphological parallelisms of the bulla and auditory ossicles in some insectivores and marsupials. *Fieldiana Zoology, 51*, 169–205.

Sinclair, W. J. (1906). Mammalia of the Santa Cruz beds. Marsupialia. Report of the Princeton University Expedition to Patagonia, vol. 4 (pp. 333–460).

Smith, F. A., Lyons, S. K., Ernest, S. K. M., Jones, K. E., Kaufman, D. M., Dayan, T., et al. (2003). Body mass of late quaternary mammals. *Ecology, 84*, 3402.

Szalay, F. S. (1994). *Evolutionary History of the Marsupials and an Analysis of Osteological Characters*. New York: Cambridge University Press.

Szalay, F. S., & Sargis, E. J. (2001). Model-based analysis of postcranial osteology of marsupials from the Palaeocene of Itaboraí (Brazil) and the phylogenetics and biogeography of Metatheria. *Geodiversitas, 23*, 139–302.

Voss, R. S., & Jansa, S. A. (2009). Phylogenetic relationships and classification of didelphid marsupials, an extant radiation of

NewWorld metatherian mammals. *Bulletin of the American Museum of Natural History, 322*, 1–177.

West, C. D. (1985). The relationship of the spiral turns of the cochlea and the length of the basilar membrane to the range of audible frequencies in ground dwelling mammals. *Journal of the Acoustical Society of America, 77*(3), 1091–1101.

Wible, J. R. (1990). Petrosals of Late Cretaceous marsupials from North America, and a cladistic analysis of the petrosal in therian mammals. *Journal of Vertebrate Paleontology, 10*, 183–205.

Wible, J. R. (2003). On the cranial osteology of the short-tailed opossum *Monodelphis brevicaudata* (Didelphidae, Marsupialia). *Annals of the Carnegie Museum, 72*, 137–202.

Wilson, D. E., & Reeder, D. M. (1993). *Mammal species of the world* (2nd ed.). Washington: Smithsonian Institution Press.